

Descent in Symmetry during Solid State Transitions and Other Anomalies in Mixed Valence Compounds



William O. J. Boo¹, Daniell L. Mattern¹, Robert M. Metzger²

¹Department of Chemistry and Biochemistry, University of Mississippi, University, MS, USA; ²Department of Chemistry and Biochemistry, University of Alabama, Tuscaloosa, AL, USA

Correspondence to: Daniell L. Mattern, mattern@olemiss.edu

Keywords: Descent in Symmetry, Ionic Ordering, Magnetic Ordering, Magnetic Susceptibility, Reconstructive Transitions

Received: May 30, 2019

Accepted: June 27, 2019

Published: June 30, 2019

Copyright © 2019 by author(s) and Scientific Research Publishing Inc.

This work is licensed under the Creative Commons Attribution International License (CC BY 4.0).

<http://creativecommons.org/licenses/by/4.0/>



Open Access

ABSTRACT

The scope of solid-state transitions, from melting temperatures down to 4.2 K, is described for six systems: K_xVF_3 , Rb_xVF_3 , Cs_xVF_3 , K_xCrF_3 , Rb_xCrF_3 , and Cs_xCrF_3 (for $x = 0.0$ to 1.0). Connections are drawn between the compounds' compositions and structures with the various transitions and ordering events. Upon solidification from the melt and gradual cooling to room temperature, a sequential descent of symmetry appears to occur, from high-symmetry perovskite phases, through possible reconstructive transitions, to phases designated α , β , and δ , within which ionic ordering finally sets in, forming many new lower-symmetry structures. Many stable new structures are seen at room temperature. Finally, at cryogenic temperatures, magnetic ordering sets in. Other anomalies for these systems are also described. The analysis underscores the overall correspondence of structure, composition, and magnetic properties in these compounds. This lowering of symmetry mirrors what has been chronicled for oxygen-bearing perovskites that have yielded so many high-temperature ceramic superconductors.

1. HISTORICAL NOTE

William O. J. Boo was a professor of chemistry at the University of Mississippi from 1967 to 1992. He died on 7 September, 2011, leaving unfinished this manuscript which reviews his two decades of research in the lower-valence fluorides of vanadium and chromium. The manuscript has been completed by two of his former colleagues, Daniell L. Mattern and Robert M. Metzger. Professor Boo also had a long-standing interest in symmetry, constructing hook-and-loop-edged polygons to teach geometry symmetry principles to elementary-school students, including tilings, solid shapes, and packings as shown in [Figure 4](#) below.

2. INTRODUCTION

This study reviews the structures, transitions, ionic and magnetic ordering phenomena, and other anomalous behaviors of six lower-valence fluorides of vanadium and chromium, A_xMF_3 , designated as $A_xM_X^{II}M_{1-x}^{III}F_3$ (A_xMF_3), where $A = K, Rb, \text{ or } Cs$; $M = V \text{ or } Cr$; and $x = 0.0 - 1.0$. Descent in symmetry in oxygen-containing perovskites was reviewed by Goodenough [1] decades before the ceramic superconductors $La_{2-x}CuO_4$ [2] and $YBaCuO_{7-x}$ [3] were discovered within that family [4]. A recent article describes how charge ordering in lanthanide cuprates is related to unusual collective behavior, such as antiferromagnetism and superconductivity [5].

The alkali metal ions K^+ , Rb^+ , and Cs^+ (the A^+ ions) demonstrate the effects of their sizes and concentrations on crystal structures. V^{2+} , V^{3+} , Cr^{2+} , and Cr^{3+} are first-row transition-metal ions with simple 3d electronic configurations. The F^- ion is small and has small polarizability. It is a weak field ligand (compared to the O^{2-} ion), and the V and Cr ions, which are octahedrally coordinated by F^- ions, have high-spin electronic configurations (Figure 1). M-F bonds have mostly ionic character, but their covalency is strong enough to form 3-D network structures.

On the other hand, due to the weak bonding in the network, the structures easily adapt to the sizes and concentrations of the A^+ ions. Hence, the corner-sharing MF_6 octahedra are flexible enough to give rise to a variety of closed-network structures [6]. The weak covalency of the M-F bonds also facilitates super-exchange interactions between nearest-neighbor magnetic centers.

Figure 2 outlines the temperature regions in which the various transitions appear to be occurring. At first, perovskite-like solid phases apparently form from the melt [7]. Upon cooling, new structures are formed, designated α , β , and δ [8-10]; when these are cooled further, ionic ordering sets in [7, 11-15]. Such transitions are characteristic of mixed-valence compounds [1, 16]. Three ordered structures are possible in the α -phases, three in the β -phases, and two in the δ -phases [7]. At very low temperatures (below 50 K), magnetic ordering sets in [11-14]. These transformations correspond to a descent in symmetry during the phase changes, from averaged and mixed-valent arrangements to more ordered ones.

Some anomalies are associated with specific phases, such as the metamagnetic transition that occurs with $K_{0.49}VF_3$ [11]. In addition, behaviors associated with specific ions occur, such as the orbital quenching of V^{3+} [11].

In the remainder of this paper, we will describe the melting temperatures of the compounds, and then detail descriptions of the reconstructive transitions and the ionic and magnetic ordering that sets in as the temperature is lowered.

3. MELTING TEMPERATURES

The melting temperatures of the A_xMF_3 compounds [7] are shown in Figure 3. Remarkably, the A_xCrF_3 compounds all melt 200° lower than their A_xVF_3 analogs. The other striking feature of Figure 3 is that the melting temperature vs. x plots of the A_xMF_3 systems are all linear. These plots include the binary parent compounds VF_3 and CrF_3 , which have cubic perovskite-like structures at high temperatures [7, 17]. This suggests that the A_xMF_3 compounds also initially solidify to cubic-perovskite-like structures.

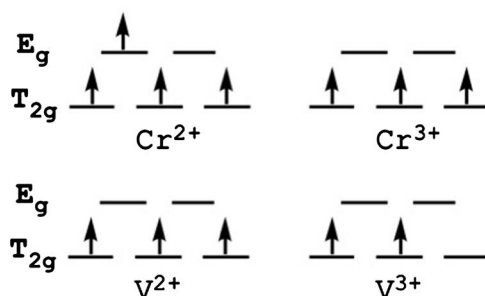


Figure 1. Electronic configurations of V^{2+} , V^{3+} , Cr^{2+} , and Cr^{3+} in a weak octahedral field.

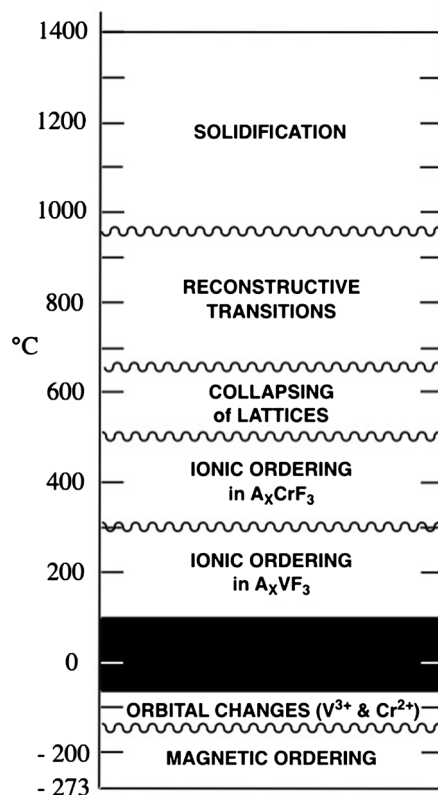


Figure 2. Temperature regimes for various likely ordering phenomena of the A_xMF_3 compounds. The wavy lines and the interpretation of the ordering processes above room temperature have partial support from DTA transitions [7].

4. RECONSTRUCTIVE TRANSITIONS

The high-temperature DTA data [7] suggest (Figure 2) a succession of reconstructive transitions between 900°C and 650°C , that break up the perovskite structure and form new lattices, designated α , β , and δ [1]. Such α , β , and δ phases have only been reported for first-row transition-metal fluorides. (Note that MF_3 and AMF_3 [18] are not mixed-valence compounds, and do not undergo reconstructive transitions. The variety of crystal structures of metal fluorides has been recently reviewed. [19]) Since a perovskite phase does form upon solidification [7, 17], we surmise that single crystals of the lower-symmetry α , β , and δ phases will grow at temperatures considerably below the solidification temperatures.

The structural analogs of the A_xMF_3 compounds [7] include: cubic perovskite (SrTiO_3) and rhenium oxide (ReO_3) ($x = 1.0$, γ phase, each belonging to space group $\text{Pm}\bar{3}\text{m} = \#221$) [20]; hexagonal tungsten bronze (HTB) ($x = 0.167$ to $x = 0.31$, α phase, space group $\text{P6}_3/\text{mcm} = \#185$) [21]; tetragonal tungsten bronze (TTB) ($x = 0.45$ to $x = 0.60$, β phase, space group $\text{P4}/\text{mbm} = \#127$) [22] or hexagonal BaTa_2O_6 ($x = 0.43$ to $x = 0.52$, β phase, space group $\text{P6}/\text{mmm} = \#191$) [21], which is a structure similar to TTB [23]; and finally modified pyrochlore (MP) ($x = 0.45$ to $x = 0.58$, δ phase, space group $\text{Fd}\bar{3}\text{m} = \#227$) [24]. The value of x alone cannot discriminate between the β phase and the δ phase [7].

The structures of the A_xMF_3 compounds have topologies which can be described using packings of simple geometrical shapes: cubic perovskite with a packing of cubes; HTB with a packing of triangular and hexagonal prisms in the ratio 2:1 (Figure 4(a)); TTB with triangular, square, and distorted pentagonal prisms 2:1:2 (Figure 4(b)); and MP with a packing of tetrahedra and truncated tetrahedra 1:1 (Figure 4(c)). Each of the packings is used in the same way. The transition metal ions are located on all vertices, the F^- ions approximately in the centers of all edges, and the A^+ ions in the centers of some or all of the 3-dimensional holes.

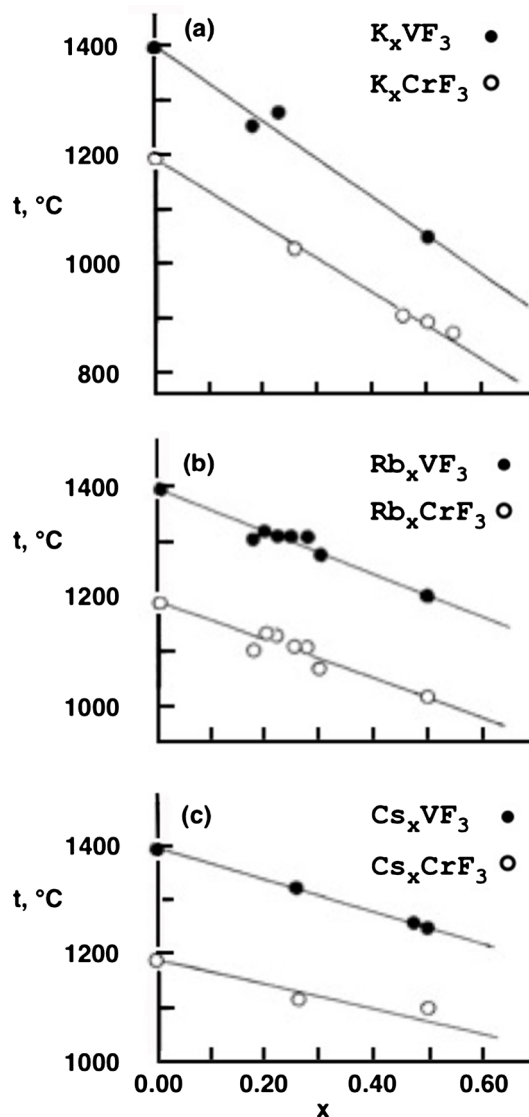


Figure 3. Melting temperatures ($^{\circ}\text{C}$) of the A_xMF_3 compounds. Data from ref [7].

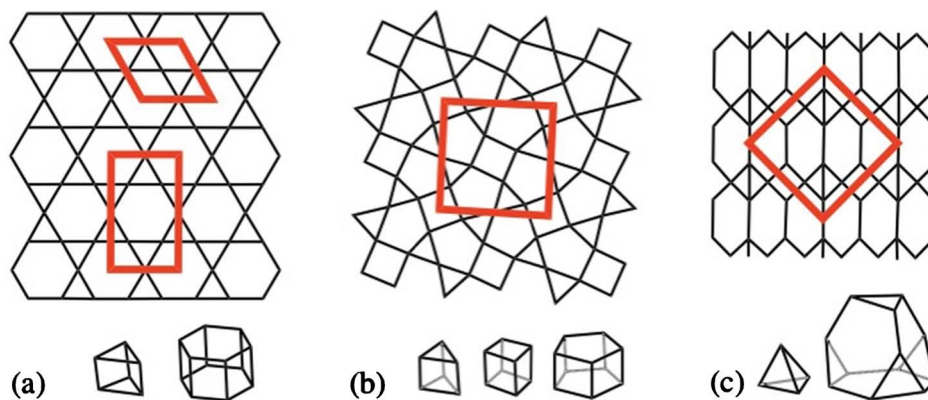


Figure 4. Geometrical configurations of (a) the HTB structure, showing the hexagonal unit cell (upper) and the ortho-hexagonal unit cell (lower); (b) the TTB structure, showing the tetragonal unit cell; and (c) the MP structure, showing the cubic unit cell.

A packing of cubes is a regular packing; a (1:1)—(tetrahedron:truncated-tetrahedron) packing is quasi-regular, while a (2:1)—(triangular-prism:hexagonal-prism) packing is semi-regular. The significance is that in each of these geometrical packings, the vertices (where transition metal ions reside) are congruent. The packing of triangular prisms, square prisms, and distorted pentagonal prisms has two sets of vertices, but all of the edges are of equal length. These packings each reveal that the MF_6 ($M = V, Cr$) octahedra share corners with six other octahedra, and all M-F-M bond angles are approximately 180° .

VF_3 and CrF_3 have lattices that collapse from cubic to rhombohedral near $500^\circ C$ [7, 25]. These are not reconstructive transitions, since their network structures are displaced, but not broken.

5. IONIC ORDERING

When they are cooled further, the A_xMF_3 compounds likely experience a variety of ionic ordering phenomena [7]. The space-group symmetries of the ordered structures are sub-groups of the α , β , or δ parent structures [26].

In the A_xCrF_3 compounds, ionic ordering includes (Cr^{2+}/Cr^{3+}) electronic ordering, ordering of partially-filled A^+ sites, and (Cr^{2+}) Jahn-Teller ordering. These ordering phenomena probably occur cooperatively between $500^\circ C$ and $300^\circ C$. The A_xVF_3 compounds undergo (V^{2+}/V^{3+}) charge ordering, ordering of partially filled A^+ sites, and (V^{3+}) Jahn-Teller ordering between $300^\circ C$ and $100^\circ C$ [7].

Three modulated structures are possible in the α phases: these correspond to 1/2-filled A^+ sites ($x = 0.167$, space group $Pnmm$ # 58); 2/3-filled A^+ sites ($x = 0.222$, space group $Cmcm$ #63); and 3/4-filled A^+ sites ($x = 0.250$, space group $Pmma$ #51) [12, 13]. The α (0.222) and α (0.250) structures only form if samples are cooled slowly; α (0.167), however, is more tenacious, and forms no matter how rapidly the samples are cooled. Table 1 lists which modulated structures form in each of the six systems. The Jahn-Teller ions

Table 1. Modulated structures and distortion ratios $\left[a/(3^{1/2}b) \right]$ in the α -phases (hettotype of HTB).

At least in the Cr salts, note the “Goldilocks” effect, where the K^+ ion is too small $\left\{ a/(3^{1/2}b) > 1 \right\}$, and Cs^+ is too large $\left\{ a/(3^{1/2}b) < 1 \right\}$, but Rb^+ is just right $\left\{ a/(3^{1/2}b) \approx 1 \right\}$, to form all three modulated structures α (0.167), α (0.222), and α (0.250). Data from ref. [7].

$x =$	0.19 D_{2h}^{12} - $Pnmm$ #58	0.22 D_{2h}^{17} - $Cmcm$ #63	0.25 D_{2h}^5 - $Pmma$ #51	0.28
K_xVF_3	α (0.167) 1.007	α (0.222) 1.006	— 1.006	— 0.991
Rb_xVF_3	α (0.167) 1.005	α (0.222) 1.004	A (0.250) 0.991	— 0.992
Cs_xVF_3	— 0.997	α (0.222) 0.997	α (0.250) 0.998	— 0.998
K_xCrF_3	— 1.027	— 1.031	— 1.029	— 1.031
Rb_xCrF_3	α (0.167) 0.991	α (0.222) 0.978	α (0.250) 0.980	— 0.994
Cs_xCrF_3	— 0.987	α (0.222) 0.986	α (0.250) 0.990	— 0.987

V^{3+} and Cr^{2+} distort their α phase compounds from hexagonal to orthorhombic, even when no modulated structures are formed. The distortion of the hexagonal unit cell is expressed as $|a|/(3^{1/2}|b|)$; this ratio can be greater than, or less than, 1.000.

In the β -phases, three ionically-ordered structures are possible, in addition to the hexagonal $BaTa_2O_6$ structure. The three ordered structures are: a distorted $BaTa_2O_6$ structure (space group $Cmmm$ #47), an ordered TTB structure (space group $P4_2bc$ #106), and a distorted TTB structure (space group $Pba2$ #32) [7, 9]. In the β -phase of K_xVF_3 the ionically-ordered TTB structure forms over the range $x = 0.45 - 0.56$. Only a trace amount of the ordered $BaTa_2O_6$ structure forms near $x = 0.40$ [27]. In the β phase of K_xCrF_3 ($x = 0.43 - 0.59$), the hexagonal $BaTa_2O_6$ structure forms if the sample is cooled slowly [28]. If the sample is cooled rapidly, the distorted TTB structure forms, and if the sample is cooled at an intermediate rate, the hexagonal $BaTa_2O_6$ structure forms at low x , the distorted TTB structure forms at high x , and the ordered $BaTa_2O_6$ structure forms in the intermediate region of x [14].

In the δ -phases, the fcc MP structure plus two ionically-ordered MP structures are possible. In the ordered structures, M^{2+} ions form linear chains along the $\langle 110 \rangle$ direction and M^{3+} ions form linear chains along the $\langle 110 \rangle$ direction. One of the ordered structures is body-centered orthorhombic MP (space group $Imma$ #74). The second ordered structure is distorted to primitive orthorhombic MP (space group $Pmna$ #53). The δ -phase of Rb_xVF_3 ($x = 0.45 - 0.52$) has the fcc structure at $x = 0.45$ and the primitive orthorhombic structure for x above 0.45. In the δ -phase of Cs_xVF_3 ($x = 0.45 - 0.52$), the fcc structure exists below $x = 0.50$ but the body-centered orthorhombic structure occurs above $x = 0.50$. The phases of Rb_xCrF_3 ($x = 0.45 - 0.56$) and Cs_xCrF_3 ($x = 0.46 - 0.54$) have primitive orthorhombic structures over their entire range of x [7].

6. ORBITAL QUENCHING OF THE V^{3+} ION

The Curie-Weiss law may be stated as:

$$\chi_M = C_M / (T - \theta)$$

where χ_M is the molar magnetic susceptibility, C_M is the Curie constant, θ is the Weiss constant, and T is the absolute temperature. A plot of $1/\chi_M$ vs T usually displays a linear region for paramagnetic compounds, with the slope of that region equal to C_M^{-1} . For VF_3 however, the plot displays 2 linear regions [29], because the orbital magnetic moment of V^{3+} is only partially quenched at high temperatures, but is totally quenched below 122 K. This phenomenon occurs in some (but not all) of the A_xVF_3 compounds as well [15]. A plot of $1/\chi_M$ vs T for $K_{0.25}VF_3$, shown in Figure 5, is an example of a compound in which the orbital

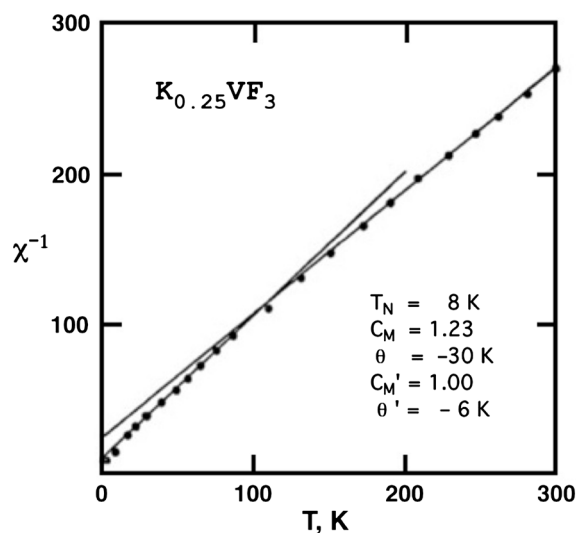


Figure 5. χ_M^{-1} versus T of $K_{0.25}VF_3$. Data from ref [15].

moment of V^{3+} becomes totally quenched near 100 K.

For the A_xVF_3 compounds, $C_M = x C_M [+2] + (1 - x) C_M [+3]$, where $C_M [+2]$ and $C_M [+3]$ are the V^{2+} and V^{3+} components of C_M , respectively. When the V^{3+} ion is totally quenched, the value of C_M falls on a straight line that connects $C_M(VF_3)$ at $x = 0.0$ with $C_M(AVF_3)$ at $x = 1.0$. **Figure 6** shows plots of C_M vs x for K_xVF_3 , Rb_xVF_3 , and Cs_xVF_3 in which C_M values were obtained from the temperature region 50 to 150 K. **Figure 6** clearly shows that the V^{3+} orbitals in the α phases are totally quenched, those in the β phases remain partially quenched, and those in the δ phases become totally quenched if they have the fcc structure, but remain only partially quenched if they have the body centered or primitive orthorhombic structures.

7. EXCITATION OF A SECOND ORBITAL STATE OF Cr^{2+}

In CrF_2 a second orbital state approximately 116 cm^{-1} above the ground orbital state was observed [30]. This excitation appears as a shoulder in a $C(\text{mag})$ vs T plot near 80 K, which leads to an additional $Rln2$ contribution to $S(\text{mag})$, making the total $S(\text{mag})$ $Rln10$ rather than $Rln5$. The magnetic susceptibility of CrF_2 emulates those of the β phase K_xCrF_3 compounds, see **Figure 7** [14]. Evidence of Cr^{2+} in these compounds behaving the same as in CrF_2 , however, is inconclusive.

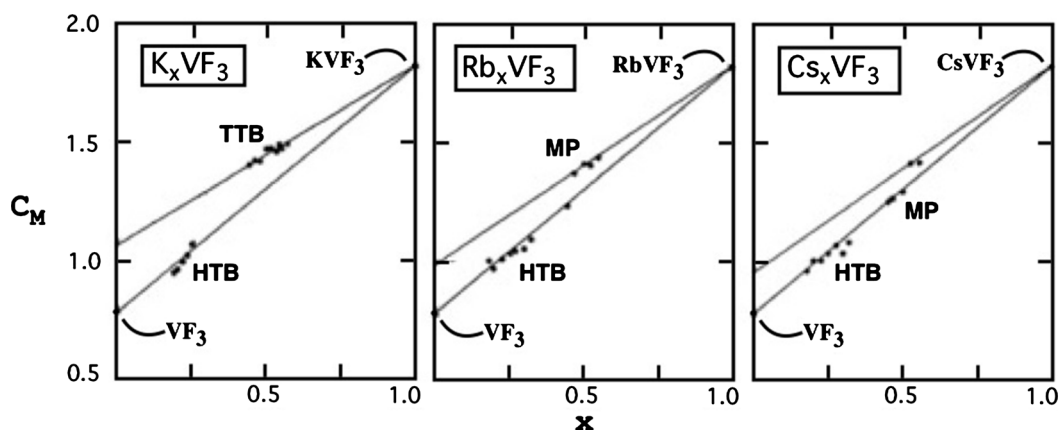


Figure 6. C_M below 150 K versus x of the A_xVF_3 compounds. Data from refs [13, 14].

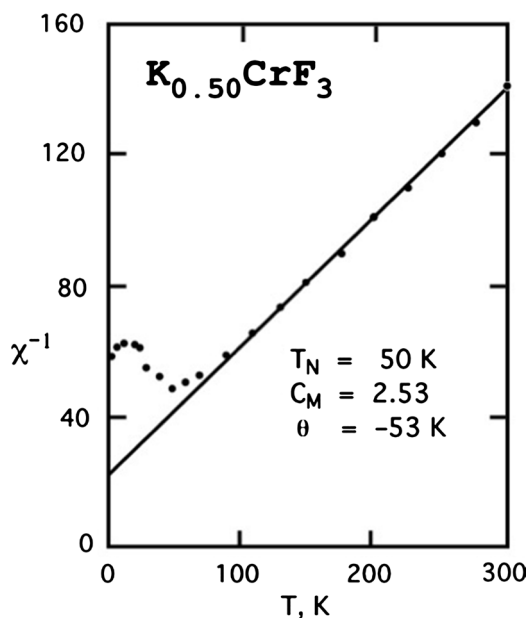


Figure 7. χ_M^{-1} versus T for $K_{0.50}CrF_3$. Data from ref [14].

8. MAGNETIC ORDERING

Magnetic interactions in the A_xMF_3 compounds are primarily antiferromagnetic, and weak ferromagnetic interactions are often difficult to detect in these complex structures. There are four observable magnetic parameters: C_M (the Curie constant), T_C (the Curie temperature), θ (the Weiss constant), and σ_0 (the spontaneous magnetic moment extrapolated to 0 K).

The C_M values of the A_xVF_3 compounds below 150 K are shown in Figure 6. Observed C_M values of the A_xCrF_3 compounds are in good agreement with calculated spin-only values, except for the α (0.167) structure of Rb_xCrF_3 [13] and the β -phase of K_xCrF_3 [14] (both at temperatures below 150 K). Possible explanations were given in the previous section for K_xCrF_3 and have been discussed before for α (0.167) of Rb_xCrF_3 [13].

The T_C value, the temperature at which long range magnetic ordering sets in, is usually seen as a maximum in a χ_M vs T plot. Most of the A_xMF_3 compounds, however, display small spontaneous magnetic moments (σ) that mask these maxima. In these cases, T_C is determined by the onset of σ . Figure 8 shows

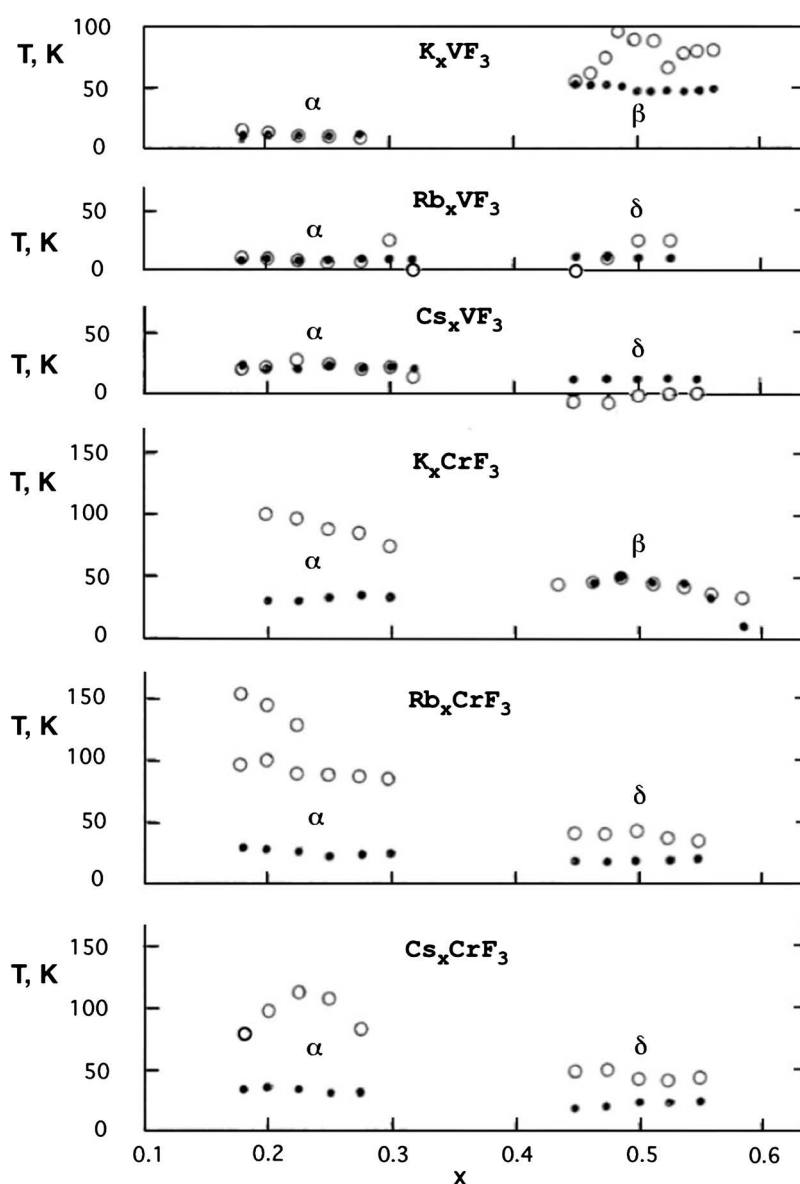


Figure 8. T_N (●) and $-\theta$ (○) for the six A_xMF_3 systems. Data from ref [13-15].

T_C and $-\theta$ values of the six systems. In general, the T_C values of the A_xVF_3 compounds are lower than their A_xCrF_3 analogs. The substitution of different A^+ ions appear to have little effect on the magnetic properties. The three structures of the β phase of K_xCrF_3 have unique T_C values: the hexagonal $BaTa_2O_6$ structure shows no evidence of T_C ; for the ordered $BaTa_2O_6$ structure, $T_C = 50$ K; and for the distorted TTB structure, $T_C = 10$ K. The T_C values of the other phases appear to be essentially constant over their entire range of x .

θ values provide a measure of the strength and sign of magnetic interactions at temperatures above T_N . Except for the β phases of K_xCrF_3 , $|\theta|$ values of the Cr compounds are greater than their V analogs. The $|\theta|$ values of the α -phases of Cr are remarkably large compared with the β and δ -phases of Cr. $Rb_{0.167}CrF_3$ displays two θ values, θ from the high temperature region and θ' from the low temperature region. The Heisenberg model [31] states that for ferromagnetic materials, $T_C = \theta$, and that for antiferromagnetic materials, $T_N = -\theta$. The latter appears to be the case for most of the A_xVF_3 compounds. However, magnetic frustrations present in the structures of α , β , and δ should suppress T_N values, making them much smaller than $|\theta|$ values [32, 33]. This is the case with some of the β -phase compounds of K_xVF_3 and all of the A_xCrF_3 compounds, except those of the β -phase of K_xCrF_3 . For antiferromagnetic interactions θ values are negative; for ferromagnetic interactions θ is positive. Overall, the Cr compounds display antiferromagnetic behavior, but the V compounds may possess a mixture of ferromagnetic and antiferromagnetic coupling.

Spontaneous magnetic moments in zero field (σ_0), extrapolated to 0 K for the six A_xMF_3 systems, are illustrated in Figure 9. The figure shows two kinds of spontaneous magnetic moments: ferromagnetic moments, shown as black areas, and ferrimagnetic moments, shown as hatched areas. The compounds which display no spontaneous moments are antiferromagnetic, and are shown as blank areas.

The V and Cr compounds show important differences in their magnetically ordered states. In these compounds, ferromagnetic order occurs from the canting of ordered spins; ferrimagnetic order means M^{2+}

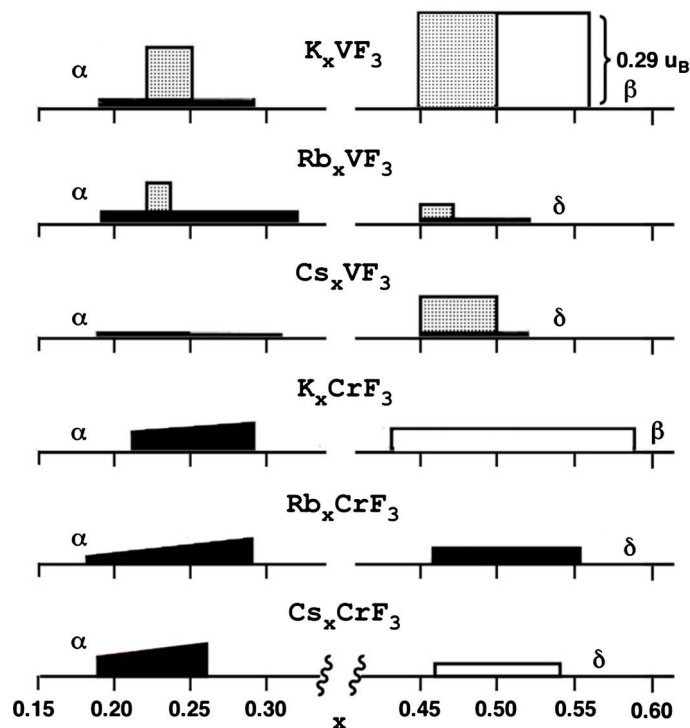


Figure 9. Spontaneous magnetic moments in zero field, extrapolated to 0 K, of the A_xMF_3 systems. Hatched areas correspond to ferrimagnetic compositions/phases, black areas to ferromagnetic compositions/phases caused by canting of spins, and blank areas represent compositions which have zero spontaneous magnetization. Data from refs [11-15].

spins are up while M^{3+} spins are down; and antiferromagnetic order means half of M^{2+} spins are up, half down, while half of M^{3+} spins are up, half down. Ferromagnetic ordering occurs in the α phases of all of the compounds and in the δ -phases of Rb_xVF_3 , Cs_xVF_3 , and Rb_xCrF_3 . The V compounds demonstrate ferrimagnetic ordering in the α (0.222) structures of K_xVF_3 and Rb_xVF_3 , in the β -phase of K_xVF_3 below $x = 0.49$, and in the fcc structure of the δ -phases of Rb_xVF_3 and Cs_xVF_3 , but no ferrimagnetic ordering was observed in any Cr compound. The β -phase of K_xCrF_3 and the δ -phase of Cs_xCrF_3 are antiferromagnetic over their range of x ; the K_xVF_3 β -phase is antiferromagnetic above $x = 0.49$.

The ferrimagnetic mechanism of the β -phase of K_xVF_3 was described in detail previously, [11] as was that of the α (0.222) structure in K_xVF_3 and Rb_xVF_3 [12]. In the δ -phases of Rb_xVF_3 and Cs_xVF_3 ferrimagnetism occurs only in the fcc structure.

MF_6 octahedra are canted in the HTB structure and the MP structure, but in the HTB and $BaTa_2O_6$ structures, there is no canting of the octahedra. The canting of spins (shown in [Figure 9](#)) is consistent with the canting of octahedra, except for the δ -phase of Cs_xCrF_3 , which, strangely enough, has no spontaneous moment. In general, the canting of spins is greater in the Cr compounds. Most notably, canting within the Cr α -phases increases with x .

9. CONCLUDING REMARKS

This paper identifies the solid-state transitions of the mixed valence A_xMF_3 compounds from their respective melting temperatures down to 4.2 K. This summary is organized to show connections of composition and structure with transitions and other events. The transitions occur in the following order:

melting \rightarrow cubic perovskite $\rightarrow \alpha, \beta, \delta \rightarrow$ ionic order \rightarrow orbital quenching of $V^{3+} \rightarrow$
 \rightarrow magnetic order.

Other features and events include:

- the V compounds melting 200° higher than their Cr analogs;
- the V compounds undergoing ionic ordering 200° lower than their Cr analogs;
- single geometric structure;
- variations of orbital quenching of V^{3+} ;
- differences of β -phases of V and Cr;
- differences of $-\theta/T_N$ of V and Cr;
- metamagnetic transition of $K_{0.49}VF_3$;
- array of different magnetic interactions;
- canting of magnetic spins.

The study of the A_xMF_3 compounds is a good introduction to an uncharted area of solid-state chemistry. Hopefully, similar studies of other systems will follow. The future breadth and depth of solid-state chemistry will be determined by the curiosity, creativity, and perseverance of solid-state chemists. High-quality powder diffraction data followed by a careful Rietveld analysis, or else crystal structure determinations (if and when crystals are obtained) should in the future buttress the arguments made here about the inferred onset of charge ordering as the symmetry is lowered. The lower-valence transition metal fluorides may ultimately yield exciting new phenomena complementary to the overwhelming success of the lower-valence transition metal oxides. Now that both Paul Hagemuller and his competitor William Boo are gone, the next generation of chemists will hopefully pick up the challenge.

ACKNOWLEDGEMENTS

This work was supported by the National Science Foundation and the University of Mississippi. We thank Prof. Jared Allred for helpful discussions.

CONFLICTS OF INTEREST

The authors declare no conflicts of interest regarding the publication of this paper.

REFERENCES

1. Goodenough, J.B. and Longo, J.M. (1970) Crystallographic and Magnetic Properties of Perovskites and Perovskite-Related Compounds. In: Hellwege, K.-H., Ed., *Landolt-Börnstein Numerical Data and Functional Relationships in Science and Technology, New Series. Group III: Crystal and Solid State Physics. Vol. 4, Magnetic and Other Properties of Oxides and Related Compounds, Part A*, Springer, Berlin, Heidelberg, New York.
2. Bednorz, J.G. and Müller, K.A. (1986) Possible High T_c Superconductivity in the Ba-La-Cu-O System. *Zeitschrift für Physik B Condensed Matter*, **64**, 189-193. <https://doi.org/10.1007/BF01303701>
3. Wu, M.K., Ashburn, J.R., Torng, C.J., Hor, P.H., Meng, R.L., Gao, L., Huang, Z.J., Wang, Y.G. and Chu, C.W. (1987) Superconductivity at 93 K in a New Mixed-Phase Y-Ba-Cu-O Compound System at Ambient Pressure. *Physical Review Letters*, **58**, 908-910. <https://doi.org/10.1103/PhysRevLett.58.908>
4. Metzger, R.M. (1988) High-Temperature Superconductivity—The First Two Years. Gordon and Breach, New York.
5. Kang, M., Pellicciari, J., Frano, A., Breznay, N., Schierle, E., Weschke, E., Sutarto, R., He, F., Shafer, P., Arenholz, E., Chen, M., Zhang, K., Ruiz, A., Hao, Z., Lewin, S., Analytis, J., Krockenberger, Y., Yamamoto, H., Das, T. and Comin, R. (2019) Evolution of Charge Order Topology across a Magnetic Phase Transition in Cuprate Superconductors. *Nature Physics*, **15**, 335-340. <https://doi.org/10.1038/s41567-018-0401-8>
6. Hagenmuller, P. (1985) Inorganic Solid Fluorides. Academic Press Inc., New York, 77-203.
7. Yeh, Y.K., Hong, Y.S., Boo, W.O.J. and Mattern, D.L. (2005) High-Temperature DTA Studies of A_xMF_3 Compounds (A=K, Rb, Cs; M=V, Cr; and $x=0-1.0$). *Journal of Solid State Chemistry*, **178**, 2191-2196. <https://doi.org/10.1016/j.jssc.2005.04.028>
8. Dumora, D., Ravez, I. and Hagenmuller, P. (1972) Les séries M_xCrF_3 (M = élément alcalin). *Journal of Solid State Chemistry*, **5**, 35-39. [https://doi.org/10.1016/0022-4596\(72\)90005-9](https://doi.org/10.1016/0022-4596(72)90005-9)
9. Cros, C., Feurer, R., Pouchard, M. and Hagenmuller, P. (1975) Les bronzes fluores de vanadium. *Materials Research Bulletin*, **10**, 383-391. [https://doi.org/10.1016/0025-5408\(75\)90009-4](https://doi.org/10.1016/0025-5408(75)90009-4)
10. Hong, Y.S., Williamson, R.F. and Boo, W.O.J. (1979) Lower Valence Fluorides of Vanadium. 3. Structures of the Pseudohexagonal A_xVF_3 Phases (Where A = Potassium, Rubidium, Thallium, or Cesium). *Inorganic Chemistry*, **18**, 2123-2125. <https://doi.org/10.1021/ic50198a013>
11. Hong, Y.S., Williamson, R.F. and Boo, W.O.J. (1980) Lower Valence Fluorides of Vanadium. 5. Dependence of Structure and Magnetic Properties of Tetragonal K_xVF_3 on Composition. *Inorganic Chemistry*, **19**, 2229-2233. <https://doi.org/10.1021/ic50210a006>
12. Hong, Y.S., Williamson, R.F. and Boo, W.O.J. (1981) Lower Valence Fluorides of Vanadium. 6. Dependence of Structure and Magnetic Properties of the Pseudohexagonal A_xVF_3 Compounds on Composition. *Inorganic Chemistry*, **20**, 403-409. <https://doi.org/10.1021/ic50216a017>
13. Hong, Y.S., Baker, K.N., Williamson, R.F. and Boo, W.O.J. (1984) Lower Valence Fluorides of Chromium. 1. The Hexagonal Bronze Type Phase Rubidium Chromium Fluoride (Rb_xCrF_3). *Inorganic Chemistry*, **23**, 2787-2793. <https://doi.org/10.1021/ic00186a015>
14. Hong, Y.S., Baker, K.N., Shah, A.V., Williamson, R.F. and Boo, W.O.J. (1990) Lower Valence Fluorides of Chromium. 2. The Phase Potassium Chromium Fluoride ($K_{0.43-0.59}CrF_3$). *Inorganic Chemistry*, **29**, 3037-3041. <https://doi.org/10.1021/ic00341a036>
15. Hong, Y.S. (1980) The Dependence of Structural and Magnetic Properties of $A(x)$ Vanadium-Trifluoride Compounds on Composition. Ph.D. Dissertation, University of Mississippi, Oxford, MS.
16. Robin M.B. and Day, P. (1967) Mixed Valence Chemistry: A Survey and Classification. In: Emeleus, H.J. and Sharpe, A.G., Eds., *Advances in Inorganic Chemistry and Radiochemistry*, Vol. 10, Academic Press, New York,

247-422. [https://doi.org/10.1016/S0065-2792\(08\)60179-X](https://doi.org/10.1016/S0065-2792(08)60179-X)

17. Hagemmuller, P. (1985) *Inorganic Solid Fluorides*. Academic Press Inc., New York, 94-96.
18. Xiao, Y., Su, Y., Li, H.-F., Kumar, C.M.N., Mittal, R., Persson, J., Senyshyn, A., Gross, K. and Brueckel, T. (2010) Neutron Diffraction Investigation of the Crystal and Magnetic Structures in KCrF_3 Perovskite. *Physical Review B*, **82**, Article ID: 094437. <https://doi.org/10.1103/PhysRevB.82.094437>
19. Leblanc, M., Maisonneuve, V. and Tressaud, A. (2015) Crystal Chemistry and Selected Physical Properties of Inorganic Fluorides and Oxide-Fluorides. *Chemical Reviews*, **115**, 1191-1254. <https://doi.org/10.1021/cr500173c>
20. Wells, A.F. (1962) *Structural Inorganic Chemistry*. Oxford University Press, London, 495.
21. Magnéli, A. (1953) Studies on the Hexagonal Tungsten Bronzes of Potassium, Rubidium, and Cesium. *Acta Chemica Scandinavica*, **7**, 315-324. <https://doi.org/10.3891/acta.chem.scand.07-0315>
22. Magnéli, A. (1949) The Crystal Structure of Tetragonal Potassium Tungsten Bronze. *Arkiv för Kemi*, **1**, 213-221.
23. Layden, G.K. (1968) Dielectric and Structure Studies of Hexagonal BaTa_2O_6 . *Materials Research Bulletin*, **31**, 349-359. [https://doi.org/10.1016/0025-5408\(68\)90006-8](https://doi.org/10.1016/0025-5408(68)90006-8)
24. Babel, D., Pausewang, G. and Viebahn, W.Z. (1967) Die Struktur einiger Fluoride, Oxide und Oxidfluoride AMe_2X_6 ; Der RbNiCrF_6 -Typ. *Zeitschrift für Naturforschung B*, **22**, 1219-1220. <https://doi.org/10.1515/znb-1967-1126>
25. Sturm, B.J. (1962) Phase Equilibria in the System Chromium (II) Fluoride-Chromium (III) Fluoride. *Inorganic Chemistry*, **1**, 665-672. <https://doi.org/10.1021/ic50003a043>
26. Boo, W.O.J. and Mattern, D.L. (2008) Concomitant Ordering and Symmetry Lowering. *Journal of Chemical Education*, **85**, 710-717. <https://doi.org/10.1021/ed085p710>
27. Williamson, R.F. and Boo, W.O.J. (1977) Lower Valence Fluorides of Vanadium. 2. Characterization of the Tetragonal Phase K_xVF_3 . *Inorganic Chemistry*, **16**, 649-651. <https://doi.org/10.1021/ic50169a031>
28. Dumora, D., Ravez, J. and Hagemmuller, P. (1970) K_xCrF_3 Series. *Bulletin de la Société Chimique de France*, 1751-1752.
29. Gossard, A.C., Guggenheim, K.L., Hsu, F.S.L. and Sherwood, R.C. (1971) Magnetic Ordering of VF_3 . *AIP Conference Proceedings*, **5**, 302-306. <https://doi.org/10.1063/1.3699445>
30. Boo, W.O.J. and Stout, J.W. (1979) Heat Capacity and Entropy of CuF_2 and CrF_2 from 10 to 300 °K. Anomalies Associated with Magnetic Ordering and Evaluation of Magnetic Contributions to the Heat Capacity. *The Journal of Chemical Physics*, **71**, 9-16. <https://doi.org/10.1063/1.438064>
31. Kittel, C. (1967) *Introduction to Solid State Physics*. 3rd Edition, John Wiley & Sons, Inc., New York, 456.
32. Hagemmuller, P. (1985) *Inorganic Solid Fluorides*. Academic Press Inc., New York, 395-413.
33. Hong, Y.S., Williamson, R.F. and Boo, W.O.J. (1980) Some Lower Valence Vanadium Fluorides: Their Crystal Distortions, Domain Structures, Modulated Structures, Ferrimagnetism, and Composition Dependence. *Journal of Chemical Education*, **57**, 583-587. <https://doi.org/10.1021/ed057p583>